J|A|C|S
ARTICLES
Published on Web 04/09/2004

Structure Determination of the Intramolecular Charge Transfer State in Crystalline 4-(Diisopropylamino)benzonitrile from Picosecond X-ray Diffraction

Simone Techert* and Klaas A. Zachariasse*

Contribution from the Max-Planck-Institut für biophysikalische Chemie, Spektroskopie und Photochemische Kinetik, 37070 Göttingen, Germany

Received August 15, 2003; E-mail: stecher@gwdg.de; kzachar@gwdg.de

Abstract: The molecular structure of photoexcited crystalline 4-(diisopropylamino)benzonitrile (DIABN) is determined by time-resolved X-ray diffraction with a time resolution of 70 ps. Spectroscopic results suggest that an ICT state with a lifetime of 3 ns is produced after photoexcitation. According to structural refinement of the X-ray data (powder diffraction), the torsional angle of the diisopropylamino group with respect to the plane of the phenyl ring of DIABN decreases from 14° in the electronic ground state to 10° in the equilibrated ICT state.

Introduction

Since the discovery of the dual fluorescence of 4-(dimethylamino)benzonitrile (DMABN) by Lippert et al. in 1959,[1,2] the structure of its intramolecular charge transfer (ICT) state has been under continuous discussion. Whereas Lippert described the ICT structure in terms of a quinoidal and hence planar resonance structure,[1,2] the emphasis of his research was on the spectral and kinetic aspects of the ICT reaction of DMABN. Grabowski et al. later focused their attention on the molecular structure of the ICT state and introduced the twisted intramolecular charge transfer (TICT) hypothesis, which claims that in the ICT state of DMABN the dimethylamino group is twisted over 90° relative to the plane of the phenyl ring and is hence electronically decoupled from the benzonitrile moiety: the principle of minimum overlap.[3−6] The locally excited (LE) state,[7] from which the ICT state is formed, was considered to be planar. The TICT model was mainly based on the fluorescence spectra of model compounds in which the amino group was forced to remain either planar (for LE) or perpendicular (for TICT) with respect to the phenyl ring.[3−6]

A direct determination of the ICT structure of DMABN or related dual fluorescent molecules is not available in the literature. As a consequence, a large number of different structures of the ICT state have been suggested since the introduction of the TICT model.[4−6,8−13] At present, predominantly the planar intramolecular charge transfer (PICT) model is discussed next to the TICT interpretation.[14−20] The PICT model claims that the amino group in the ICT state of DMABN and derivatives is not perpendicularly twisted, but that the ICT state has an overall planar structure. This hypothesis was based on experiments from which indirect information on the ICT structure was deduced.[10,11,15] In support of the PICT model, efficient ICT was observed with the planarized aminobenzonitriles 1-methyl-7-cyano-2,3,4,5-tetrahydro-1*H*-1-benzazepine (NMC7)[21,22] in diethyl ether and acetonitrile and 1-*tert*-butyl-

(1) Lippert, E.; Lüder, W.; Boos, H. In *Advances in Molecular Spectroscopy;* European Conference on Molecular Spectroscopy, Bologna, Italy, 1959; Mangini, A., Ed.; Pergamon Press: Oxford, U.K., 1962; p 443.
(2) Lippert, E.; Lüder, W.; Moll, F.; Nägele, W.; Boos, H.; Prigge, H.; Seibold-Blankenstein, I. *Angew. Chem.* **1961**, *73*, 695.
(3) Rotkiewicz, K.; Grellmann, K. H.; Grabowski, Z. R. *Chem. Phys. Lett.* **1973**, *21*, 212.
(4) Grabowski, Z. R.; Rotkiewicz, K.; Siemiarczuk, A.; Cowley, D. J.; Baumann, W. *Nouv. J. Chim.* **1979**, *3*, 443.
(5) Lippert, E.; Rettig, W.; Bonačič-Koutecký, V.; Heisel, F.; Miehé, J. A. *Adv. Chem. Phys.* **1987**, *68*, 1.
(6) Rettig, W.; Maus, M. In *Conformational Analysis of Molecules in Excited States*; Waluk, J., Ed.; Wiley: New York, 2000; p 1.
(7) The use of the name LE state in the ICT reaction of D/A-substituted molecules such as DMABN obviously originates from the formal kinetic similarity of the ICT reaction scheme consisting of an initially excited LE state and an ICT state and the schemes applicable to excimer and exciplex formation. Strictly speaking, the excitation is just as delocalized in the LE state as in the ICT state of molecules such as DMABN, the difference mainly residing in the degree of charge separation. When this formal kinetic analogy as the basis for the term LE is considered to be unacceptable, then it may be best to use the neutral term S_1 state.
(8) Leinhos, U.; Kühnle, W.; Zachariasse, K. A. *J. Phys. Chem.* **1991**, *95*, 2013.
(9) Grabowski, Z. R.; Dobkowski, J. *Pure Appl. Chem.* **1983**, *55*, 245.
(10) Von der Haar, Th.; Hebecker, A.; Il'ichev, Yu.; Jiang, Y.-B.; Kühnle, W.; Zachariasse, K. A. *Recl. Trav. Chim. Pays-Bas* **1995**, *114*, 430.
(11) Il'ichev, Yu., V.; Kühnle, W.; Zachariasse, K. A. *J. Phys. Chem A* **1998**, *102*, 5670.
(12) Sudholt, W.; Staib, A.; Sobolewski, A. L.; Domcke, W. *Phys. Chem. Chem. Phys.* **2000**, *2*, 4341.
(13) Zachariasse, K. A.; Grobys, M.; Tauer, E. *Chem. Phys. Lett.* **1997**, *274*, 372.
(14) Rettig, W.; Zietz, B. *Chem. Phys. Lett.* **2000**, *317*, 187.
(15) Zachariasse, K. A. *Chem. Phys. Lett.* **2000**, *320*, 8.
(16) Demeter, A.; Druzhinin, S.; George, M.; Haselbach, E.; Roulin, J.-L.; Zachariasse, K. A. *Chem. Phys. Lett.* **2000**, *323*, 351.
(17) Kwok, W. M.; Ma, C.; Matousek, P.; Parker, A. W.; Phillips, D.; Toner, W. T.; Towrie, M.; Umapathy, S. *J. Phys. Chem. A* **2001**, *105*, 984.
(18) Okamoto, H.; Inishi, H.; Nakamura, Y.; Kohtani, S.; Nakagaki, R. *J. Phys. Chem. A* **2001**, *105*, 4182.
(19) Zilberg, S.; Haas, Y. *J. Phys. Chem. A* **2002**, *106*, 1.
(20) Rappoport, D.; Furche, F. *J. Am. Chem. Soc.* **2004**, *126*, 1277.
(21) Zachariasse, K. A.; Grobys, M.; von der Haar, Th.; Hebecker, A.; Il'ichev, Yu. V.; Jiang, Y.-B.; Morawski, O.; Kühnle, W. *J. Photochem. Photobiol., A* **1996**, *102*, 59. Erratum: Zachariasse, K. A.; Grobys, M.; von der Haar, Th.; Hebecker, A.; Il'ichev, Yu. V.; Jiang, Y.-B.; Morawski, O.; Kühnle, W. *J. Photochem. Photobiol., A* **1998**, *115*, 259.

6-cyano-1,2,3,4-tetrahydroquinoline (NTC6)[23] in *n*-hexane and more polar solvents.

Similarly indirect experimental approaches to determine the ICT molecular structure have been reported which were interpreted as giving support to the TICT model. The most recent one is based on the syn−anti photoisomerization of a cyanopyridine derivative in methanol at low temperature (183 K).[24] It should be noted, however, that, in protic solvents such as methanol, the photophysics of DMABN is complicated by the appearance of a new excited state product besides the ICT species; this product has recently been attributed to hydrogen bonding with the alcohol solvent.[25−27]

Another approach to unravel the structure of the ICT state is based on time-resolved resonance Raman (TR^3)[17,28] and infrared[18,29−32] measurements. It is shown by these studies that for the ICT state of DMABN the frequency attributed to the *N*-phenyl stretch vibration shifts to lower values. From the TR^3 results[17,28] as well as from calculations of IR frequencies,[33] it was concluded that the dimethylamino group is electronically decoupled from the rest of the molecule in accordance with the TICT model. In conflict with this interpretation, however, is the observation that the quinoidal character of the phenyl ring of the DMABNs in the ICT state is larger than in the ground state, whereas a decrease in quinoidality should occur when the ICT state would have a TICT structure.[18] A general consequence of this discrepancy is that definite structural conclusions on bond lengths and molecular structure cannot be made from TR^3 and IR experiments, until fully reliable quantum chemical calculations of the transient spectra are available.[31]

To resolve this dilemma by a direct determination of the structure of the ICT state of a dual-fluorescent aminobenzonitrile, picosecond X-ray diffraction measurements were carried out with crystalline powder of 4-(diisopropylamino)benzonitrile (DIABN). This molecule was chosen because it undergoes efficient ICT in the crystalline state.[34] The ICT state of DIABN in the crystal is formed from the LE state with a rise time of 11 ps at 25 °C, a process that slows down upon cooling, to 55 ps at −110 °C.[34] The ground state crystal structure indicates that the DIABN molecules are present as pairs in a T-shaped configuration, with a head-to-head arrangement.[35]

The technique used in the present study is time-resolved X-ray powder diffraction: a pump−probe method in which an optical femtosecond laser pulse initiates a reaction in the excited state, which is consequently probed by an X-ray pulse, generated by a synchrotron of the 3rd generation (70 ps time resolution).[36,37] By varying the time delay between pump and probe pulse, a series of snapshots of the changing structure is taken, each shot probing the average molecular structure (nonexcited plus excited, including the dispersion of the latter) at a given time. Such experiments make it possible to monitor structural changes of short-lived intermediates during chemical[37−41] and biochemical[42,43] photoreactions, since the X-ray pulse directly probes its molecular structure. Powder diffraction rather than single crystal diffraction was chosen, to guarantee a coincidence of the penetration depth of the optical laser pulse with the X-ray probe pulse. The present experiments were carried out at the time-resolved beamline ID09B of the European Synchrotron Radiation Facility (ESRF) in Grenoble.

Time-resolved X-ray diffraction with single crystals in the millisecond and microsecond time regime[44,45] as well as in the picosecond time regime[41] have been reported. Investigations of structural changes of metal−ligand electron-transfer systems in the liquid-phase applying EXAFS methods have also been carried out.[46,47]

Experimental Section

Sample Preparation. DIABN was synthesized and purified as described previously.[16,34] The molecular structure of DIABN is shown as an insert in Figure 1. Crystals were grown from ethanol solution by slow evaporation. Two kinds of powder samples were used in the experiments: first, the crunched powder of DIABN was dispersed on a 5−20 μm thick mica plate (the single grains did not exceed thicknesses of 500 nm), with a layer thickness not exceeding 5−40 μm. Such a thickness guarantees that samples with an optical density of at most 1.2 are transparent at the excitation wavelength (267 nm). In a second preparation method, DIABN was directly sublimed onto the mica plates. In contrast to Kapton foil, which can alternatively be used in powder diffraction experiments,[48] mica is not destroyed by the UV pump light during the present experiments. Additional Bragg diffraction signals coming from the mica were masked in the data treatment procedure. The occurrence of preferred orientations in the samples was

(22) Zachariasse, K. A.; Grobys, M.; von der Haar, Th.; Hebecker, A.; Il'ichev, Yu. V.; Morawski, O.; Rückert, I.; Kühnle, W. *J. Photochem. Photobiol., A* **1997**, *105*, 373.
(23) Zachariasse, K. A.; Druzhinin, S. I.; Bosch, W.; Machinek, R. *J. Am. Chem. Soc.* **2004**, *126*, 1705.
(24) Dobkowski, J.; Wójcik, J.; Koźminski, W.; Kołos, R.; Waluk, J.; Michl, J. *J. Am. Chem. Soc.* **2002**, *124*, 2406.
(25) Kwok, W. M.; George, M. W.; Grills, D. C.; Ma, C.; Matousek, P.; Parker, A. W.; Phillips, D.; Toner, W. T. Towrie, M. *Angew. Chem., Int. Ed.* **2003**, *42*, 1826.
(26) Kwok, W. M.; Ma, C.; George, M. W.; Grills, D. C.; Matousek, P.; Parker, A. W.; Phillips, D.; Toner, W. T. Towrie, M. *Phys. Chem. Chem. Phys.* **2003**, *5*, 1043.
(27) Zachariasse, K. A.; Yoshihara, T.; Druzhinin, S. I. *J. Phys. Chem. A* **2002**, *106*, 6325. Erratum: Zachariasse, K. A.; Yoshihara, T.; Druzhinin, S. I. *J. Phys. Chem. A* **2002**, *106*, 8978.
(28) Ma, C.; Kwok, W. M.; Matousek, P.; Parker, A. W.; Phillips, D.; Toner, W. T.; Towrie, M. *J. Phys. Chem. A* **2002**, *106*, 3294 and references cited there.
(29) Okamoto, H.; Inishi, H.; Nakamura, Y.; Kohtani, S.; Nakagaki, R. *Chem. Phys.* **2000**, *260*, 193.
(30) Okamoto, H.; Kinoshita, M. *J. Phys Chem. A* **2002**, *106*, 3485.
(31) Okamoto, H.; Kinoshita, M.; Kohtani, S.; Nakagaki, R.; Zachariasse, K. A. *Bull. Chem. Soc. Jpn.* **2002**, *75*, 957.
(32) Chudoba, C.; Kummrow, A.; Dreyer, J.; Stenger, J.; Nibbering E. T. J.; Elsaesser, T.; Zachariasse, K. A. *Chem. Phys. Lett.* **1999**, *309*, 357.
(33) Dreyer, J.; Kummrow, A. *J. Am. Chem. Soc.* **2000**, *122*, 2577.
(34) Druzhinin, S. I.; Demeter, A.; Zachariasse, K. A. *Chem. Phys. Lett.* **2001**, *347*, 421.
(35) Kocher, N.; Noltemeyer, M.; Stalke, D.; Druzhinin, S. I.; Zachariasse, K. A., in preparation.
(36) Schotte. F.; Techert, S.; Anfinrud, P.; Srajer, V.; Moffat, K.; Wulff, M. In *Third-Generation Hard X-ray Synchrotron Radiation Sources*; Mills, D. M., Ed.; Wiley-Interscience: New York, 2001, p 345.
(37) Techert, S.; Schotte, F.; Wulff, M. *Phys. Rev. Lett.* **2001**, *86*, 2030.
(38) Neutze, R.; Wouts, R.; Techert, S.; Kirrander, A.; Davidson, J.; Kocsis, M.; Schotte, F.; Wulff, M. *Phys. Rev. Lett.* **2001**, *87*, 195508.
(39) Geis, A.; Block, D.; Bouriau, M.; Schotte, F.; Techert, S.; Plech, A.; Wulff, M.; Trommsdorff, H. P. *J. Lumin.* **2001**, *94*, 493.
(40) Busse, G.; Tschentscher, Th.; Plech, A.; Wulff, M.; Frederichs, B.; Techert, S. *Faraday Discuss.* **2002**, *122*, 105.
(41) Collet, E.; Lemée-Cailleau, M.-H.; Buron-Le Cointe, M.; Cailleau, H.; Wulff, M.; Luty, T.; Koshihara, S.-Y.; Meyer, M.; Toupet, L.; Rabiller, P.; Techert, S. *Science* **2003**, *300*, 612.
(42) Srajer, V.; Teng, T.-Y.; Ursby, T.; Pradevard, C.; Ren, Z.; Adachi, S.; Schildkamp, W.; Bourgeois, D.; Wulff, M.; Moffat, K. *Science* **1996**, *274*, 1726.
(43) Ren, Z.; Perman, B.; Srajer, V.; Teng, T.-Y.; Pradervand, C.; Bourgeois, D.; Schotte, F.; Ursby, T.; Kort, R.; Wulff, M.; Moffat, K. *Biochemistry* **2001**, *40*, 13788.
(44) Coppens, P.; Novozhilova, I.; Kovalevsky, A. *Chem. Rev.* **2002**, *102*, 861.
(45) Kim, C. D.; Pillet, S.; Wu, G.; Fullagar, W. K.; Coppens, P. *Acta Crystallogr.* **2002**, *A58*, 133.
(46) Chen, L. X.; Jäger, W. J. H.; Jennings, G.; Gosztola, D. J.; Munkholm, A.; Hessler, J. P. *Science* **2001**, *292*, 262.
(47) Chen L. X.; Jennings G.; Liu T.; Gosztola D. J.; Hessler J. P.; Scaltrito D. V.; Meyer G. J. *J. Am. Chem. Soc.* **2002**, *124*, 10861.
(48) Klug, H. P.; Alexander, L. E. *X-ray Diffraction Procedures*, 2nd ed.; John Wiley: New York, 1974 and references therein.

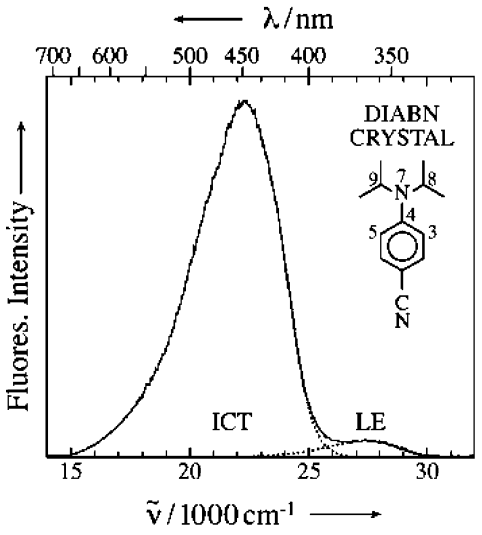

Figure 1. Fluorescence spectrum of crystalline 4-(diisopropylamino)-benzonitrile (DIABN) with the molecular structure of DIABN as an insert. The spectral subtraction of the locally excited (LE) and intramolecular charge transfer (ICT) emission bands, see text, has been carried out by using the LE fluorescence spectrum of 4-(dimethylamino)benzonitrile (DMABN).

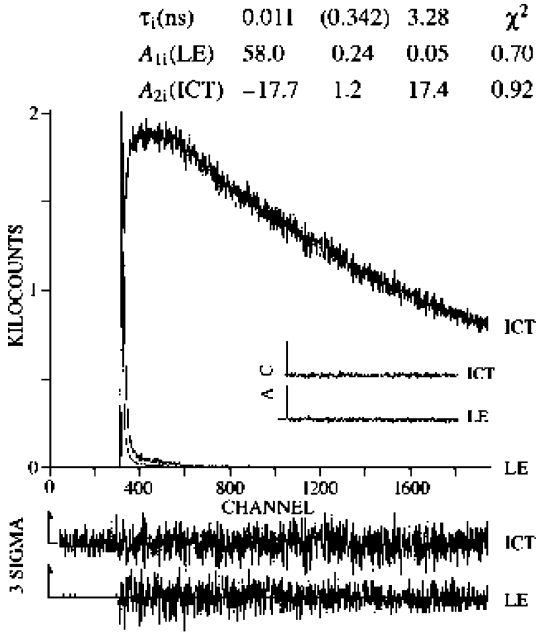

Figure 2. LE and ICT fluorescence response functions of crystalline 4-(diisopropylamino)-benzonitrile (DIABN) on mica at 25 °C. The LE and ICT decays are analyzed simultaneously (global analysis). The decay times (τ_2, τ_1) and their preexponential factors A_{1i} and A_{2i} are given (eqs 1 and 2). The shortest decay time τ_2 is listed first. The time in parentheses is attributed to crystal defects (see ref 34). The weighted deviations, expressed in σ (expected deviations), the autocorrelation functions $A-C$, and the values for χ^2 are also indicated. Excitation wavelength: 279 nm. Time per channel: 1.978 ps.

checked by comparing the intensity distribution of the various Bragg peaks of the powder sample of DIABN on mica with that of powder samples in capillaries, in which the microcrystals are assumed to be randomly oriented. This comparison was made with a separate experiment during which the capillaries are rotated.[37] Preferred orientations were not found. As a matter of fact, an overall preferred orientation will not influence the signal from the excited state species under investigation, as difference maps and relative changes under dark and light conditions are compared.

Spectroscopic Characterization. The emission spectra of solid DIABN were measured by using a ISA-SPEX Fluorolog 3-22 fluorometer. Fluorescence decay times were determined with a picosecond time-correlated single photon counting (SPC) apparatus described previously.[16,34] The samples that were used for the fluorescence measurements were also employed for the time-resolved X-ray diffraction experiments.

Time-Resolved X-ray Diffraction Experiments. The data for the time-resolved X-ray diffraction (XRD) experiments were collected at the ID09B beamline of the ESRF. The setup at ID09B follows a classical optical pump/X-ray probe scheme as explained elsewhere.[36] The pump wavelength of the mode-locked Ti:Sapphire laser, which runs synchronously with single pulses of the X-rays (probe), was generated by frequency tripling to $\lambda_{exc} = 267$ nm. The laser power was attenuated to $5-8$ μJ with a pulse width of 100 fs. The laser beam was focused down to a diameter of $200-400$ μm. Higher laser power as well as tighter focus led to a visible photochemical degradation of the DIABN sample. The X-ray probe pulses were selected from the 16-bunch filling mode of the storage ring using a synchronized chopper. For a pulse width of 70 ps (X-ray) a flux on the sample of 0.5 to 2×10^8 photons (s 100 mA)$^{-1}$ was obtained in a 200×200 μm^2 focal spot. The monochromatic X-ray probe beam at 16.5 keV (λ(X-ray) = 0.753 Å) was selected by a Si_{111} monochromator. Diffraction data were collected with a MAR133 CCD camera (diameter = 133 mm, pxl-size = 64.7×64.7 μm^2) with varying sample-to-detector distances of $120-160$ mm depending on the desired resolution of the powder diffraction pattern. The exposure time was 10 min. During the measurements, the decay of the storage ring current was monitored online and later included in the intensity correction of the diffraction pattern. The XRD experiments were carried out at room temperature. The laser and X-ray beams hit the sample in a quasiparallel configuration resulting in an optimal overlap between pump and probe volume. The XRD experiments were carried out at room temperature. The overall heating of the sample could be determined from the 2θ shift of the Bragg peak maxima by comparing the diffraction pattern under light illumination-with the dark diffraction pattern. The sample heating was found to be negligible. At the beginning of a measurement cycle, time zero ($t = 0$) was set by monitoring the pulse sequence of the direct laser and the X-ray beam by using a fast GaAs detector. For negative times ($t < 0$), the X-ray pulse arrives before the laser pulse, whereas for positive times the X-ray pulse arrives after the laser pulse. The time zero setting was accurate within 30 ps (jitter (X-ray-laser pulse) = 3 ps). The repetition frequency of the stroboscopic experiment was 897 Hz.

To reach a signal-to-noise ratio of the diffraction data sufficient for reliable data treatment, about 5% of the DIABN sample was optically excited. In addition, the excitation of the powder should be as homogeneous as possible, because of the difference in the cross section of the scattered X-ray photons (ca. 10^{-15} cm^{-2}) as compared with the cross section of the optical photons (ca. 10^{-13} cm^{-2}). When using organic molecules containing phenyl moieties such as DIABN, the optical density of the material can easily reach a value of $4-5$ for a 100 μm thick crystal in the UV spectral range, which results in a low penetration depth for the optical photons and therefore in a small nonhomogeneous excitation yield. When using UV light for pumping this kind of material, it is therefore better to work with powdered samples or microcrystals rather than with single crystals in the micrometer range. The time-resolution of the present diffraction experiments is limited by the X-ray pulse width (70 ps). Further details of the experimental setup have been described elsewhere.[36−38,40]

Results and Discussion

Fluorescence Spectra and Decay Times. Spectroscopic Characterization. The fluorescence spectrum of crystalline DIABN at 25 °C, excited at 270 nm, is shown in Figure 1. In this spectrum, the emission band of the locally excited (LE) state has a maximum around 27700 cm^{-1}, whereas the strongly red-shifted intramolecular charge transfer (ICT) fluorescence

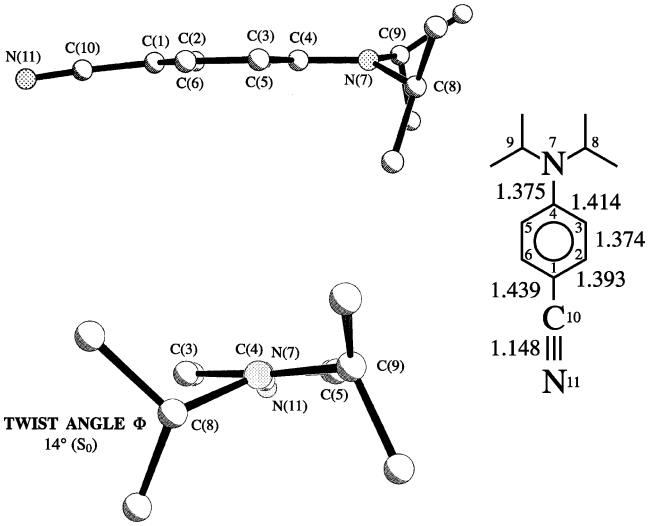

Figure 3. Molecular structure of 4-(diisopropylamino)benzonitrile (DIABN) represented by a side view and a view along the N7−C10 axis. The bond lengths (in Å) have been indicated in the molecular formula. The twist angle Φ is defined by eq 3 in the text.

band peaks at 22300 cm^{-1}. The ICT to LE fluorescence quantum yield ratio Φ′(ICT)/Φ(LE) has a value of 26.7. The global analysis of the LE and ICT fluorescence decay curves of the crystalline DIABN on mica at 25 °C is presented in Figure 2. The decay curves are defined as

$$i_f(\mathrm{LE}) = A_{11}\exp(-t/\tau_1) + A_{12}\exp(-t/\tau_2) \quad \text{with } A = A_{12}/A_{11} \quad (1)$$

$$i_f(\mathrm{ICT}) = A_{21}\exp(-t/\tau_1) + A_{22}\exp(-t/\tau_2) \quad (2)$$

The longest fluorescence decay time (3.28 ns), measured at the emission ICT maximum, agrees reasonably well with the value of 2.92 ns reported earlier for crystalline DIABN at this temperature.[34] For DIABN on mica, the growing-in time of 11 ps (Figure 2) was likewise reproduced. This time is that of the LE → ICT reaction. Note that the time of 11 ps is smaller than the time-resolution of the present laser pump/X-ray probe setup (ca. 70 ps).

Crystal Structure of DIABN in the Ground State. The molecular structure of DIABN, as determined by X-ray analysis in the ground state,[16,35] is depicted in Figure 3. An important feature emerging from this structure is the value of 14° for the twist angle Φ. The data for the bond lengths and the torsional angle Φ have been averaged over the two DIABN molecules in the asymmetric unit.[35] The angle Φ is defined via the dihedral angles φ_1' and φ_1'' (eq 3).

$$\Phi = (\varphi_1 + \varphi_2)/2 = (\varphi_1' + \varphi_1'' + \varphi_2' + \varphi_2'')/4 \quad (3)$$

In eq 3, φ_1' is the dihedral angle between the atoms C5−C4−N7−C8 of Figure 3, φ_1'' is the dihedral angle C3−C4−N7−C9, and φ_1 is the torsional angle of one DIABN molecule of the asymmetric unit. φ_2', φ_2'', and φ_2 are defined in a similar manner for the second DIABN molecule in the asymmetric unit.

X-ray Diffraction Experiments. Data Processing. One-dimensional diffraction patterns of DIABN powder were obtained by integrating the two-dimensional images, detected by the MAR detector, with the program package Fit2d.[49] These patterns were normalized against the background signal. The analysis of an integrated one-dimensional diffraction pattern of DIABN is shown in Figure 4, which will be explained in more detail in the following section.

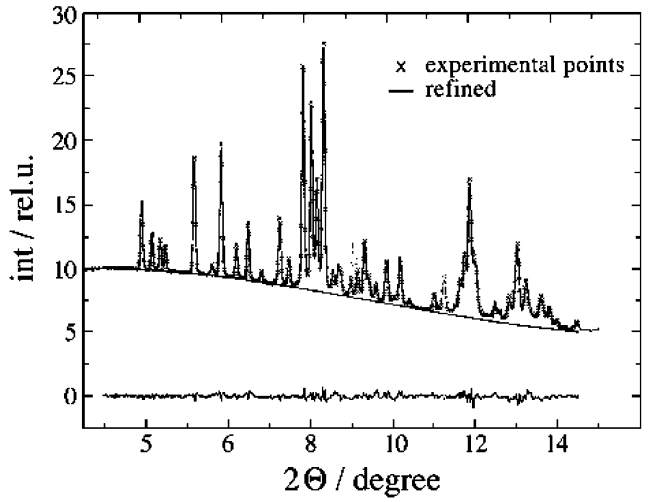

Figure 4. Integrated powder diffraction pattern of DIABN at $t = 70$ ps.

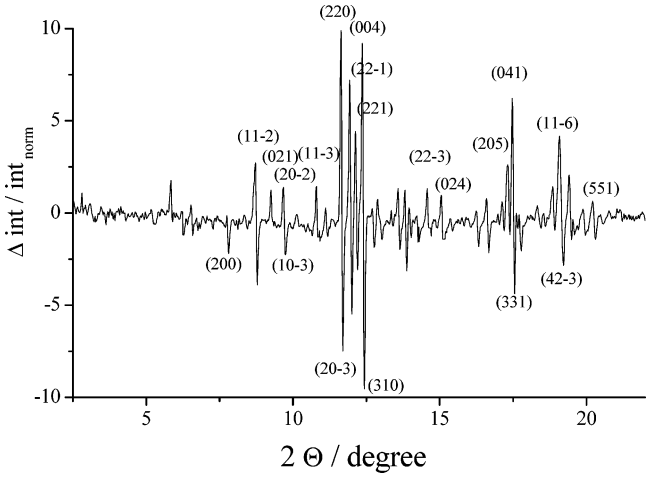

Figure 5. Difference map for photoexcited DIABN ($t = 70$ to -150 ps).

The intensities of the difference signal Δ(int) of the photoexcited state of DIABN (Figure 5) are obtained by subtracting the intensities of the partially excited crystalline material from those of the nonexcited powder in the electronic ground state. To do so, the data for $t = \infty$ were taken at a time where the laser arrived just after the X-rays ($t = -150$ ps). These data were compared with those at positive times, at which the laser pulse arrived just before the X-rays. An example for a normalized intensity difference at one time *t* (one time point of the intensity correlation function) is shown in Figure 5. After laser excitation at $t = 70$ ps, the diffraction signal originates from a mixture of ground state molecules and excited state molecules. However, in the difference map, the nonexcited molecules in the unit cells do not contribute to the difference signal. The most prominent Bragg reflection changes in Figure 5 are marked by their Miller indices *hkl*. The intensity changes range between 1% and 8% of the total signal. The fact that these intensity changes take place in the positive as well as in the

(49) Hammersley, A. P.; Svensson, M.; Hanfland, M.; Fitch, A. N.; Haeusermann, D. *High Pressure Res.* **1996**, *14*, 235.

negative direction shows that the effects observed in the present experiments with DIABN are not due to sample heating (see above). In such a case, the intensity differences would only be negative, due to an increase of the peak width resulting from an increase of the Debye−Waller factor.[41] The difference map also shows that radiation damage, such as the increase of amorphous background or the gradual decrease of diffraction amplitudes, was not observed and hence does not take place, notwithstanding the repetition frequency of the experiment of 897 Hz (see above).

To treat the time-resolved diffraction data quantitatively, three assumptions have to be made: (a) the photoexcitation of DIABN in the crystal lattice is purely statistical; (b) it is possible, within the time resolution of the experiments, to separate lattice movements such as translations and librations from structural changes of the molecular system; (c) the population decay of the photoexcited molecules in the singlet excited state takes place on a much longer time scale than the intramolecular structural reorganization, which is considered to be instantaneous.

Statistical Excitation of DIABN Molecules. Essential for the data treatment of photoexcited DIABN powder is the assumption of statistical excitation of the molecules in the periodic crystal lattice. Taking into consideration that the number of optical photons N^{ph} is equal to or larger than the number of absorbed photons $N^{ph}_{abs}(= N^{m}_{exc})$, one can write for the number of photoexcited molecules N^{m}_{exc}

$$N^{m}_{exc} = \sigma_{abs} N^{m} \quad \text{with } N^{ph} > N^{ph}_{abs} = N^{m}_{exc} \tag{4}$$

where σ_{abs} is the absorption cross section and N^{m} is the number of molecules in the crystal volume. Note that only in the case of a localized (not excitonic) excitation, one absorbed photon results in one distorted molecule (or asymmetric unit), for which the structure can be refined. The following definitions are used: defect molecules for the distorted photoexcited molecules, defect structure for their structure, and N_{def} for the number of photoexcited molecules of which the structure is refined, def being an abbreviation for defect. With these definitions, the equality $N^{m}_{exc} = N_{def}$ holds.

Since the local photoinduced disorder in the DIABN crystal is statistical and can be treated as originating from structural defects, the representative refined cell of the photoexcited phase is also statistical. Therefore, N_{def} expresses the probability that a certain site will be occupied by a given distorted photoexcited molecule. During the refinement, the photoexcited phase is considered to have the crystallochemical formula *DIABN$_x$ where the subscript x describes the stoichiometry of the photoexcited phase as percentage of all molecules in the powder sample. The whole lattice is then DIABN$_{1-x}$*DIABN$_x$, and DIABN$_{1-x}$ stands for the percentage stoichiometry of the nonphotoexcited phase of the powder. The subscripts $1-x$ and x are hence directly proportional to N_{def}. On the basis of these definitions, the number of nonexcited (nondefect = ndef) molecules N_{ndef} is equal to $N_{ndef} = 1 - N_{def}$.

During the data treatment based on the present statistical approach, information on long range order such as periodic fluctuations of distorted structures in the crystal lattice is evidently lost. This situation differs from, for example, 1-dimensional electron conductors,[41] for which, through a so-called domino effect, the photoinduced structural changes lead to the formation of completely new subdomains in the crystal lattice.

Decay of the ICT Excited State of Crystalline DIABN. Time-Dependent Correlation Function. It is assumed that intra- and intermolecular degrees of freedom (DOFs) are separable in the DIABN crystal lattice. Under this condition, the position of a Bragg diffraction peak is a property of the translational lattice and is related to acoustic and optical low frequency phonon modes. The intensity of a Bragg diffraction peak, on the other hand, depends on the scattering properties of the atoms (scattering factor) and the molecular geometry of the system. In the following, a derivation is presented of the time correlation function, which exactly expresses this time-dependence of the Bragg diffraction peaks as a function of geometrical changes in the DIABN molecule and the occupancy of the excited state.

The correlation function $C_n(t)$, describing the time course of the modulated intensity signal of the nth Bragg diffraction peak, can be expressed as

$$C_n(t) = \frac{I(\theta, t) - I(\theta, t = \infty)}{I(\theta, t = 0) - I(\theta, t = \infty)} \tag{5}$$

where $I(\theta, t)$ is the intensity of the nth Bragg peak at the position 2θ and the time t. The correlation function is normalized against the intensity of the same Bragg peak at $t = 0$ and $t = \infty$. $t = 0$ defines the starting time of the reaction and $t = \infty$ indicates the end of the reaction at time infinity, which represents the stationary case of the product distribution.

For a photophysical reaction, the decay of the occupancy of a defect structure (such as the ICT state DIABN$_{def}$) is a single exponential, when a reversible reaction in the excited state does not occur from this excited state. For the ICT state of crystalline DIABN (Figure 2), the decay can be considered as a single exponential, as the rise-time of 11 ps is not resolved within the time resolution of the present X-ray diffraction experiment. The total reaction as such, however, is reversible in the crystallographic sense, which means that the recovery of the ground state depletion is 100% efficient and that the molecular nature of the reactant, from which the photophysical process starts, is equal to that of the product.

Assuming a monoexponential decay, the occupancy of the defect structure in eq 4 is

$$^{1}N_{def}(t) = {}^{1}N_{def}(t = 0) \exp(-k_{N_{def}} t) \tag{6}$$

$^{1}N_{def}(t)$ is the occupancy of the defect structure for t, $^{1}N_{def}(t = 0)$ is the occupancy for $t = 0$, and $k_{N_{def}}$ is the rate constant of the defect occupancy.

In addition, for the time-dependence of the structure factor $|F_{hkl}(t)|^2$, an Arrhenius expression can be adopted

$$|F_{hkl}(t)|^2 = |F_{hkl}(t = 0)|^2 \exp(-k_{F_{hkl}} t) \tag{7}$$

In an analogous manner, $F_{hkl}(t)$ is the structure factor at the time t, $F_{hkl}(t = 0)$ is this factor at $t = 0$, and $k_{F_{hkl}}$ is the rate constant of the structural changes, i.e., the change in the structure factor.

The correlation function $C_n(t)$ of eq 5 then leads to eq 8. Details on the development of this correlation function will be

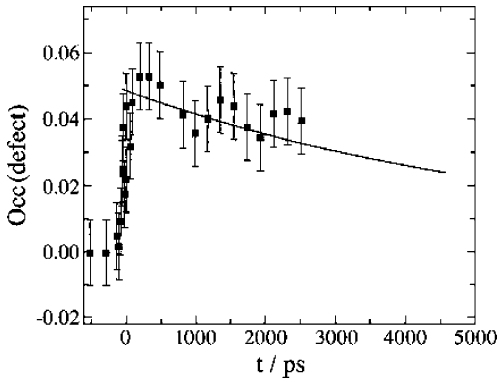

Figure 6. Time course of the occupancy of the photoinduced defect-structure of DIABN.

reported elsewhere.[50]

$$C_n(t) = \sum_{hkl} \exp(-k_{N_{\text{def}}} t) \exp(-k_{F_{hkl}} t) = \sum_{hkl} \bar{U}_{N_{\text{def}}} \bar{U}_{F_{hkl}} \quad (8)$$

$\bar{U}_{N_{\text{def}}}$ and $\bar{U}_{F_{hkl}}$ are the time matrices for the time dependence of the occupancy change and the time dependence of the structural changes or changes in the structure factor.

In the case of crystalline DIABN, the transient state is populated within the time resolution of the experiment. Under this condition, $|F_{hkl}(t = 0)|^2$ changes with a step function at $t = 0$; $\bar{U}_{F_{hkl}}$ of the time correlation function then acts as a constant offset or as a step function and $C_n(t)$ is predominantly modulated through $\bar{U}_{N_{\text{def}}}$ which characterizes the decay of the defect structure population.

$$C_n(t) = \text{const} \sum_{hkl} \exp(-k_{N_{\text{def}}} t) \quad (9)$$

The data for the occupancy of the light-distorted DIABN molecules ${}^1N_{\text{def}}(t)$ in Figure 6 have been fitted by using eq 9. ${}^1N_{\text{def}}(t)$ is a result of the refinement of the powder diffraction pattern for all times t. The procedure for the occupancy and structure refinement of photoexcited DIABN will be explained in the following section. For clarity, the dynamical aspects of the data are discussed first.

From the data in Figure 6, a rate constant $k_{N_{\text{def}}} = 9.2 \times 10^6$ s^{-1} is obtained by applying eq 9 to the decay of the refined occupancy (eq 6). This corresponds to a single-exponential decay with a decay time of 6.3 (±2.8) ns. This time is longer than the fluorescence decay time of 3.28 ns observed for the ICT state of DIABN powder (Figure 2). Taking into account the error limits for the fit in Figure 6, the decay curves can be considered to describe the same transient species, the ICT state of DIABN. A possible reason for the difference in the measured decay times could be that the fluorescence intensity decay in Figure 2 is a direct measurement, whereas the refined occupancies ${}^1N_{\text{def}}(t)$ come from processed and refined data with an error bar of ±0.01−0.015 on a value of 0.05 = ${}^1N_{\text{def}}(t)$. The occupancies are normalized against 1.00 = 100% of state population. The limits of the refined occupancy values are indicated as error bars in Figure 6.

Structural Refinement of DIABN in the Excited State. The separation of the intrinsic dynamics of the structural changes in the DIABN molecules from the decay behavior of the occupancies (Figure 6) is possible if it is assumed that the population decay of the photoexcited molecules is much longer than that of the structural intramolecular reorganization effects produced by the instantaneous light excitation. Under this condition, the squared structure factor changes as a Heaviside step function at $t = 0$, which can be refined for that time. Further changes in the Bragg diffraction peak are then assigned to the population decay related to the molecular structure represented by $|F_{hkl}(t = 0)|$. See eq 7.

On the basis of the assumptions listed above, the translational and rotational DOFs and one intramolecular torsional DOF (Figure 1) in the molecular structure of photoexcited DIABN were refined. The remaining intramolecular DOFs (especially those of the benzonitrile and the diisopropylamino moieties of DIABN) were kept fixed during the refinement since they cannot be determined within the resolution of the presented powder data (and therefore do not significantly contribute to the observed signal changes). For this widely used rigid body approach, refs 36 and 48 may be consulted. On the basis of the knowledge obtained from similar systems,[37] the separation of nonrigid and rigid parts of a molecule is reasonable, since in the singlet excited state the distortions of the phenyl moiety as well as those of the CN substituent are negligibly small for 4-aminobenzonitriles. In fact, since the rigid DOFs are not large amplitude motions, it is not to be expected that they will change the intensity of the powder diffraction peaks to the same extent as observed here for DIABN. It should be emphasized that for the nonphotoexcited DIABN molecules (in the S_0 ground state) all inter- and intramolecular DOFs were held fixed during the refinement.[37]

The powder patterns of DIABN are analyzed by applying the Rietveld refinement. Program packages GSAS and Reflex/Reflex Plus (MSI) were used.[51,52] DIABN crystallizes in a monoclinic space group $C\ 2/c$ with $Z = 4$,[35] which is typical for organic molecules of this structure.[53] During the refinement, the unit cell parameters were allowed to vary in order to compensate for small variations in the sample-to-detector distance. For the unit cell, the values $a = 16.399$ (±0.001) Å, $b = 14.551$ (±0.001) Å, $c = 20.475$ (±0.001) Å, and $\beta = 92.86°$ (±0.007°) with $Z = 4$ were found (literature: $a = 16.649$ Å, $b = 14.441$ Å, $c = 20.354$ Å, and $\beta = 92.7°$).[35]

A typical refined powder pattern for DIABN at lower space resolution is shown in Figure 4 for $t = 70$ ps. The similarity between the experimental and simulated diffraction pattern is expressed by the background corrected weighted profile R-factor R_{wp} in percent ($R_{\text{wp}} = 5.7\%$ in Figure 4). The definition of R_{wp} is given in the Appendix, to be found in the Supporting Information (eq A1). The R_{wp} values of the refined pattern, which reflect the "goodness" of the refined structure and also the quality of the experimental powder diffraction pattern, are sufficiently small so that the structural disorder with respect to the intramolecular torsional angle can be refined.

As seen in Figure 7, one asymmetric unit consists of two DIABN molecules, so that the refined torsional angle Φ of the

(50) Techert, S. *J. Appl. Crystallogr.* In press.

(51) Larson, A. C.; von Dreele, R. B. *GSAS—General structure analysis system*, Program and Handbook; 86-748; Copyright Regents of the University of California: California, 1998.

(52) *Reflex/Reflex-Plus, MaterialsStudio*, Version 2.2, Program and Handbook; Accelrys Inc.: San Diego, CA, 2002.

(53) Heine, A.; Herbst-Irmer, R.; Stalke, D.; Kühnle, W.; Zachariasse, K. A. *Acta Crystallogr.* **1994**, *B50*, 363.

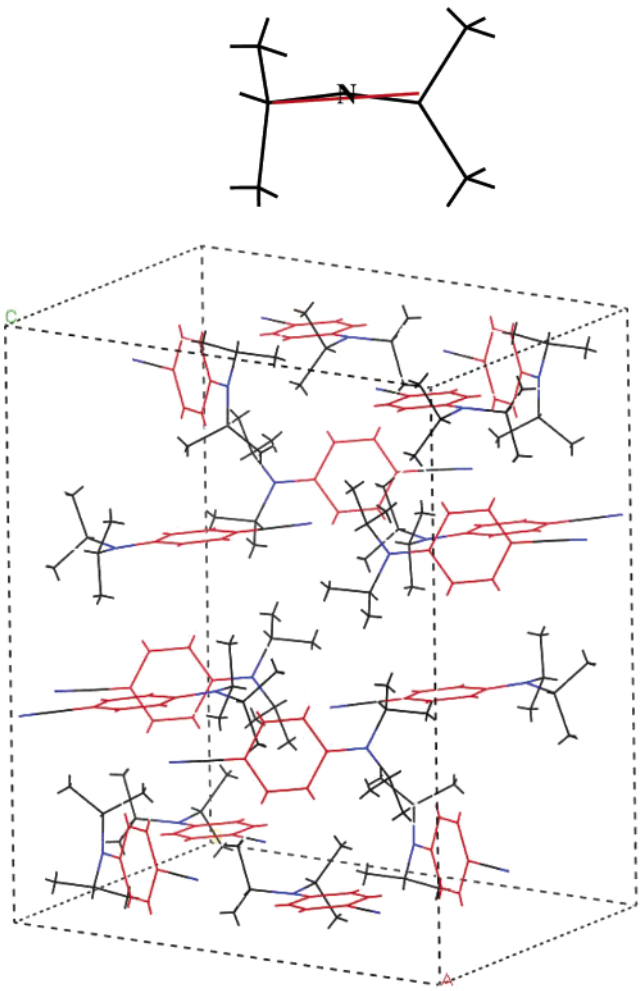

Figure 7. Top: Superposition of the structure of the ground state (black) with the structure of the excited state (red) 70 ps after photoexcitation. The twist angle of the diisopropylamino group of DIABN is shown in a view along the N7−C10 axis of the molecule (see Figure 3). Bottom: The unit cell of DIABN in a presentation, in which all molecules are in the excited state. The atoms are given in CPK colors.

diisopropylamino group with respect to the phenyl ring is an averaged torsional angle of these two subunits (eq 3).

The results of the refinement are summarized in Table 1. For the DIABN powder, a torsional angle of $\Phi = 13-14°$ was found for negative times. Within the error of the powder refinement (±1.5°), this value reproduces that determined from single crystal experiments on DIABN ($\Phi = 14.3°$)[35] showing that the same ground state structure (see Figure 3) is determined under the present experimental conditions. The torsional angle changes in a step function at $t = 0$ from $\Phi = 14°$ to 10° (±1−2°) for the photoexcited defect structure, the ICT state of DIABN. The occupancy of this defect structure was determined to be 0.05 according to the procedure defined in the section on statistical excitation. The R_{wp} values of the refined photoexcited structures ranged between 3.5% and 7% (Table 1). Note, that the angle Φ corresponds to the final twist angle of the equilibrated ICT state.

The structure of the ICT state of DIABN 70 ps after photoexcitation is depicted in Figure 7. On the bottom of Figure 7, the unit cell of DIABN is shown in a presentation mode, in which all molecules are in the excited state. Compared to the ground state structure,[35] the molecules have not changed their

Table 1. Refined Molecular Geometries and Occupancies of Photoexcited DIABN Compared to Literature Values of the Ground State[a]

t [ps]	ϕ_{tors} [deg]	occupancy	R_{wp} [%]
static	14.3	1.000	unknown[35]
−500	13.338	0.000	5.6
−250	14.2525	0.000	5.9
0	10.1768	0.025	6.2
10	11.173	0.038	5.8
70	10.0458	0.044	5.9
150	10.734	0.045	6.7
270	10.4483	0.053	6.2
415	11.2558	0.053	6.4
750	10.0923	0.045	6.7
935	10.2735	0.042	6.7
1325	10.093	0.0405	6.2
1525	10.093	0.046	6.24
1735	10.542	0.044	6.9
1945	11.3665	0.038	7.9
2365	11.2945	0.040	8.4
2580	10.881	0.012	9.95
2795	10.0935	0.011	9.34

[a] The torsional angle, ϕ_{tors}, is defined by eq 3 (see text). The uncertainty in the refined torsional angle is $\sigma(\phi_{tors}) = 1.5-2°$; the error in the occupancy $\sigma(occ) = 0.015$. 100% occupancy = 1.00.

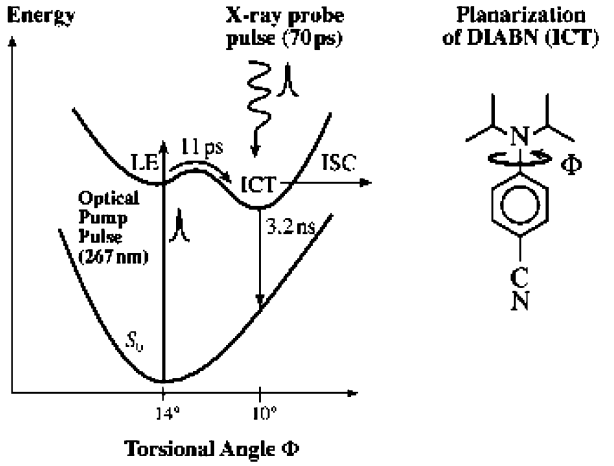

Figure 8. Photophysical pathway of photoexcited DIABN in a crystal.

position in the unit cell and the intermolecular distances between two perpendicular stacked DIABN molecules remain the same as in the ground state (5.97 Å). The intermolecular distance between two DIABN molecules in the same stack also did not change with respect to the ground state structure (10.99 Å). Figure 7, top, shows the ground state structure of DIABN in black superimposed with the excited state structure in red (70 ps after optical excitation).

In conclusion, the twist angle Φ of DIABN in the ICT state decreases from 14° to 10°, after excitation from the ground state to the ICT state, showing that the overall structure of DIABN becomes somewhat more planar in the ICT state.

The results of the present structure analysis are summarized in Figure 8. After excitation with 267 nm, the DIABN molecules in the crystal undergo internal conversion to the lowest excited singlet state of LE character S_1(LE). From this S_1(LE) state, the ICT state is formed within 11 ps at 25 °C (ICT rate constant $k_a = 9.1 \times 10^{10}$ s^{-1}). From the fluorescence decay of the ICT state (Figure 2) it follows that this state has a lifetime of 3.28 ns. Presumably, in the solid state DIABN also shows an intersystem crossing from this ICT state to a triplet state, as has been found for *n*-hexane solution.[34] As this triplet state

therefore should grow in with a time of 3.28 ns, the excited state monitored here (Figure 6) is not the triplet state of DIABN.

It is of interest to note in this connection that, for photoexcited DMABN powder, a torsional angle of 11° was found for the dimethylamino group with respect to the phenyl plane.[37] In crystalline DMABN only LE emission was observed.[34,54] Since the intermolecular distances remain unchanged as compared with the ground state (in DIABN as well as in DMABN), with relatively large intermolecular distances, structural artifacts resulting from excimer formation can be excluded.

Conclusion

Upon photoexcitation of DIABN molecules in a crystalline powder, X-ray diffraction experiments with a time resolution of 70 ps show that the torsional angle of the diisopropylamino group relative to the plane of the phenyl ring of DIABN decreases from 14° in the electronic ground state to 10° in the equilibrated ICT state. It is therefore concluded that the ICT state of DIABN in the crystal lattice has an effectively planar structure.

Acknowledgment. The time-resolved X-ray diffraction experiments reported in this work were measured at the beamline ID09B of the ESRF. In this context, the authors wish to thank Dr. M. Wulff for his strong support and interest in this work. Dr. A. Plech and W. Reichenbach are thanked for technical assistance. Prof. J. Troe is thanked for his permanent support and interest in this work. S.T. is grateful to the DFG for the research grant TE 347/1-1 and to the Aventis Foundation for the Karl von Winnacker fellowship. Thanks are also due to Dr. S.I. Druzhinin for measuring fluorescence spectra and picosecond fluorescence decays of crystalline DIABN and to Dr. M. Noltemeyer for the X-ray crystal structure of DIABN.

Supporting Information Available: Additional details in appendix form. This material is available free of charge via the Internet at http://pubs.acs.org.

JA0379518

(54) Demeter, A.; Zachariasse, K. A. *Chem. Phys. Lett.* **2003**, *380*, 699.